ISAR IMAGE RECONSTRUCTION ALGORITHM

Andon Dimitrov Lazarov
Burgas Free University

ISAR АЛГОРИТЪМ ЗА ВЪЗСТАНОВЯВАНЕ НА ОБРАЗИ

Андон Димитров Лазаров

Abstract: *This paper deals with generalized ISAR geometry and image reconstruction technique. Three-dimensional* (*3-D*) *ISAR scenario is projected on two-dimensional (2-D) radar registration plane. The arbitrary movement of the object is decomposed into two components: radial displacement of the object's geometric center and rotational movement around it. It is proven that the demodulated ISAR signal, reflected from the target during aperture synthesis, can be considered as 2-D Fourier transformation of the image function, corrected by an exponential term and as a consequence, the image function can be extracted by 2-D inverse Fourier transformation of the phase corrected ISAR signal. Numerical experiment validating aforementioned statements is performed.*

Key words*: ISAR Model, Image Reconstruction*

1. Introduction

Inverse synthetic aperture radar (ISAR) is a powerful technique for microwave imaging of targets. High-range and cross-range spatial resolutions are achieved by target illuminating with wideband pulses and by coherently integrating the echoes backscattered from different aspect angles, respectively. Several algorithms for ISAR image reconstruction have been proposed in the literature [1-8]. The simplest technique is the range-Doppler (RD), which consists of a two-dimensional inverse Fourier transform (2D-IFT) of the received signal, after motion compensation. The RD technique is successfully applicable when the effective rotation vector does not significantly change during the integration time [1, 2]. Theoretically, the cross-range resolution is inversely proportional to the variation of the target aspect angle, hence, the larger the aspect angle variation, the better the spatial resolution. In real scenarios long data sets are recorded and the target rotation vector is usually far from constant. Therefore, a suitable time windowing technique must be used in order to obtain one or more focused ISAR images. The criterion used to define the "highest focused" image is based on the definition of image contrast. It is worth suggesting the image entropy [4] as a possible candidate for measuring the image focal quality. Robust autofocus image reconstruction technique based on a parametric linear frequency modulated signal model and nonlinear least mean square minimization of a special defined cost function is suggested in [5]. A survey of different autofocus algorithm is performed in [6]. Nevertheless, a recent analysis confirms that the image contrast is a very accurate indicator for image focal quality [3, 7]. In this context in [8]

the image with the highest contrast as the optimal image is addressed, and the algorithm for the maximum-contrast-based automatic time window selection is defined and its effectiveness tested by means of computer simulations and real data, and the effect of the application of weighting windows is analyzed. In the present paper a generalized ISAR geometry and image reconstruction technique are considered. The main objectives are to analyze ISAR signal formation process and based on it to interpret image reconstruction algorithm. For this purpose a three-dimensional ISAR scenario is projected on two-dimensional 2-D radar registration plane and the arbitrary movement of the object is decomposed into two components: radial displacement of the object's geometric center and rotational movement around it. It is proven that the demodulated ISAR signal, reflected from the target during aperture synthesis, can be considered as 2-D Fourier transformation of the image function, corrected by an exponential term and as a consequence, the image function can be extracted by 2-D inverse Fourier transformation of the phase corrected ISAR signal. The rest of the paper is organized as follows. In Section 2 ISAR geometry in 2-D projection plane is described. In Section 3 ISAR signal analysis is performed. In Section 4 image reconstruction algorithm and phase correction based on 2-D entropy minimization are described. In section 5 numerical experimental results are presented. In Section 6 conclusions are made.

2. ISAR Geometry

The target is moving arbitrarily in 2-D space. The movement can be decomposed into radial displacement of the object's mass center and rotational motion with respect to mass center. At the particular moment the ISAR scenario is depicted in Fig.1, where xOy is the coordinate system of observation, translated in mass center of the object. The object is placed in 2-D coordinate grid, defined by 2-D Cartesian coordinates XOY .

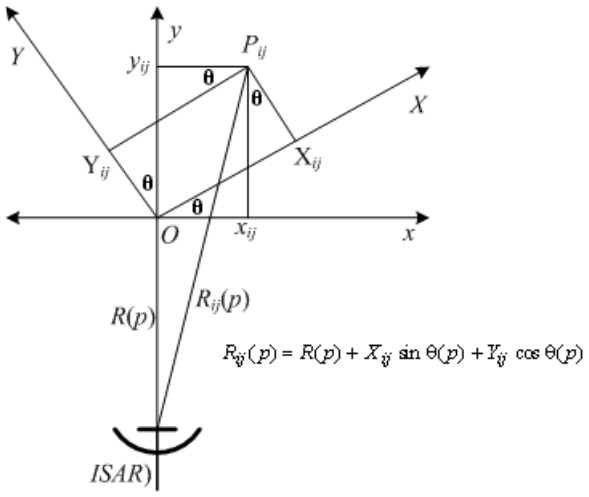

Fig. 1. 2-D ISAR geometry.

Each reference point P_{ij} from the object's space is defined by coordinates $X_{ij} = i\Delta X$, $Y_{ij} = j\Delta Y$, where i and j are indexes of discrete coordinates, ΔX and ΔY are the size of the grid's cell. Coordinates $x_{ij}(p)$ and $y_{ij}(p)$ of observation of the reference point P_{ij} and the

distance $R_{ij}(p)$ to the ISAR (point of observation) can be calculated from the geometry in Fig. 1 as follows

(1) $x_{ij}(p) = X_{ij}\cos\theta(p) - Y_{ij}\sin\theta(p)$;

(2) $y_{ij}(p) = X_{ij}\sin\theta(p) + Y_{ij}\cos\theta(p)$;

(3) $R_{ij}(p) = R(p) + X_{ij}\sin\theta(p) + Y_{ij}\cos\theta(p)$,

where $\theta(p)$ is the rotational angle of the target; $R(p)$ is the mass center displacement with respect to ISAR; $R_{ij}(\hat{t}) = R(\hat{t}) + X_{ij}\sin\theta(\hat{t}) + Y_{ij}\cos\theta(\hat{t})$, $\hat{t} = t \bmod T_p$, t is the fast time. Accept that during the fast time t the distance $R_{ij}(\hat{t})$ does not change, then the time dependence of the distance can be expressed as a function of slow time (pT_p), i.e. $R_{ij}(pT_p)$ or $R_{ij}(p)$ where p is the number of emitted pulse, T_p is the time repetition period of emitted pulses.

3. ISAR signal analysis

3.1. ISAR emitted pulse

The normalized emitted LFM pulse can be written as

(4) $$s(t) = \mathbf{rect}\frac{t}{T_0}\exp\left[j(\omega t + bt^2\right], \text{ where } \mathbf{rect}\frac{t}{T_0} = \begin{cases} 1 \text{ if } 0 \le \dfrac{t}{T_0} < 1 \\ 0 \text{ otherwise} \end{cases}$$

3.2. ISAR signal model

The signal reflected by the target and received by a radar antenna can be expressed as

(5) $$S(t) = \sum_{j=1}^{J}\sum_{i=1}^{I} a_{ij}\,\mathbf{rect}\frac{t - t_{ij}}{T_0}\exp\left\{j\left[\omega\left(t - t_{ij}\right) + b.\left(t - t_{ij}\right)^2\right]\right\}$$

where $t_{ij} = \dfrac{2R_{ij}(p)}{c}$ is the time delay of the return from ij – the point scatterer.

$$\mathbf{rect}\frac{t - t_{ij}}{T_0} = \begin{cases} 1 \text{ if } 0 \le \dfrac{t - t_{ij}}{T_0} < 1 \\ 0 \text{ otherwise} \end{cases}$$

In discrete form $$\mathbf{rect}\frac{(k_{\min} + k)\Delta T - t_{ij}}{T_0} = \begin{cases} 1 \text{ if } 0 \le \dfrac{(k_{\min} + k)\Delta T - t_{ij}}{T_0} < 1 \\ 0 \text{ otherwise} \end{cases}$$

$k_{\min} = \left\lceil \dfrac{t_{\min}}{\Delta T} \right\rceil$ where $t_{\min} = \dfrac{2R_{ij\min}}{c}$, then $k_{\min} = \left\lceil \dfrac{2R_{\min}}{c.\Delta T} \right\rceil$

Demodulation (dechirping, or deramping) of the signal return is performed by multiplication with complex conjugated amplitude of the emitted signal, i.e.

$$\hat{S}(t) = S(t) \times \mathbf{rect}\frac{t}{T_0}\exp\left[-j(\omega t + bt^2\right] =$$

(6)

$$\sum_{j=1}^{J}\sum_{i=1}^{I} a_{ij}\mathbf{rect}\frac{t-t_{ij}}{T_0}\exp\left\{j\left[\omega\left(t-t_{ij}\right)+b.\left(t-t_{ij}\right)^2\right]\right\}\times\exp\left[-j(\omega t+bt^2\right]$$

which yields

$$\hat{S}(t) = \sum_{j=1}^{J}\sum_{i=1}^{I} a_{ij}\mathbf{rect}\frac{t-t_{ij}}{T_0}\exp\left\{-j\left[(\omega+2bt)t_{ij}-bt_{ij}^2\right]\right\}. \quad (7)$$

Denote the current angular frequency of emitted LFM pulse as $\omega(t) = \omega + 2bt$, where ω is the carrier angular frequency, and b is the chirp rate. In discrete form fast time parameter can be written as $t = k\Delta T$, where k is the sample number, ΔT - the sample time duration, then the current dicretized frequency can be written as $\omega_k = \omega + 2b(k\Delta T)$ or $\omega_k = k\Delta\omega_k$ where $\Delta\omega_k = \left(\frac{\omega}{k} + 2b(\Delta T)\right)$, where $k = \overline{0, K-1}$. Then (7) can be rewritten as

$$S(k,p) = \sum_{j=1}^{J}\sum_{i=1}^{I} a_{ij}\mathbf{rect}\frac{t-t_{ij}}{T_0}\exp\left[-j\left(2\omega_k\frac{R_{ij}(p)}{c} - b\left(\frac{2R_{ij}(p)}{c}\right)^2\right)\right] \quad (8)$$

In discrete form

$$S(k,p) = \sum_{j=1}^{J}\sum_{i=1}^{I} a_{ij}\mathbf{rect}\frac{(k_{\min}+k)\Delta T - t_{ij}}{T_0}\exp\left[-j\left(2\omega_k\frac{R_{ij}(p)}{c} - b\left(\frac{2R_{ij}(p)}{c}\right)^2\right)\right] \quad (9)$$

The quadratic term $b\left(\frac{2R_{ij}(p)}{c}\right)^2$ defines the along track uncompensated slow time signal phase of the *ij*-th reference point which can be generalized for all reference points, i.e. $\phi(p) = b\left(\frac{2R_{ij}(p)}{c}\right)^2$, and removed from the sum i.e.

$$S(k,p) = \exp\left[j\phi(p)\right]\sum_{j=1}^{J}\sum_{i=1}^{I} a_{ij}\mathbf{rect}\frac{(k_{\min}+k)\Delta T - t_{ij}}{T_0}\exp\left[-j\left(2\omega_k\frac{R_{ij}(p)}{c}\right)\right] \quad (10)$$

Define $R_{ij}(p)$ by equation (3), then

$$S(k,p) = \exp\left[j\phi(p)\right]\sum_{j=1}^{J}\sum_{i=1}^{I} a_{ij}\mathbf{rect}\frac{(k_{\min}+k)\Delta T - t_{ij}}{T_0}\times \exp\left[-j2\omega_k\frac{R(p)+X_{ij}\sin\theta(p)+Y_{ij}\cos\theta(p)}{c}\right] \quad (11)$$

Like most of the existing ISAR imaging it is assumed that the coherent processing interval is short and the difference $\Delta\theta = \theta(N-1) - \theta(0)$ is small, in this case $\cos\theta(p) \approx 1$, $\sin\theta(p) = \theta(p) = p\delta\theta$, $\delta\theta$ denotes an uniform angular step.

$$S(k,p)=\exp\left[j\phi(p)\right]\sum_{j=1}^{J}\sum_{i=1}^{I} a_{ij}\,\mathbf{rect}\frac{(k_{\min}+k)\Delta T-t_{ij}}{T_0}\times \exp\left[-j\left(2\omega_k\frac{R(p)}{c}+\frac{2\omega_k\theta(p)}{c}X_{ij}+\frac{2\omega_k}{c}Y_{ij}\right)\right] \quad (12)$$

The term $2\omega_k\frac{R(p)}{c}$ does not depend on the object's discrete coordinates (*ij*) and can be placed in front of the sum, i.e.

$$S(k,p)=\exp\left[j\left(\phi(p)-\frac{2\omega_k R(p)}{c}\right)\right]\sum_{j=1}^{J}\sum_{i=1}^{I} a_{ij}\,\mathbf{rect}\frac{(k_{\min}+k)\Delta T-t_{ij}}{T_0}\times \exp\left[-j\left(\frac{2\omega_k p\delta\theta}{c}X_{ij}+\frac{2\omega_k}{c}Y_{ij}\right)\right] \quad (13)$$

Taking into account that the object's coordinates are expressed as $X_{ij}=i\Delta X$, and $Y_{ij}=j\Delta Y$, and uniform angular variation as $\theta(p)=p\delta\theta$, the following substitutions can be made

$$\frac{2\omega_k}{c}X_{ij}.\theta(p)=\frac{2\pi.p.i}{N}\text{, where } N=\frac{c}{2\Delta X.(\delta\theta)f_k},\ f_k=\frac{\omega_k}{2\pi}$$

$$\frac{2\omega_k}{c}Y_{ij}=\frac{2\pi.k.j}{K}\text{, where } K=\frac{c}{2(\Delta f_k)\Delta Y},\ (\Delta f_k)=\frac{(\Delta\omega_k)}{2\pi}$$

$$\frac{2\omega_k}{c}R(p)=\frac{2\pi k}{\frac{c}{2(\Delta f_k)}}R(p)=\phi_k(p)$$

The expression can be rewritten (13) as

$$S(k,p)=\exp\left[j\left(\phi(p)-\frac{2\omega_k R(p)}{c}\right)\right]\sum_{j=1}^{J}\sum_{i=1}^{I} a_{ij}\,\mathbf{rect}\frac{(k_{\min}+k)\Delta T-t_{ij}}{T_0}\times \exp\left[-j\left(\frac{2\pi.p.i}{N}+\frac{2\pi.k.j}{K}\right)\right] \quad (14)$$

The signal return $S(k,p)$ can be considered as a Fourier transform of the 2-D discrete complex reflectivity density function $\sum a_{ij}.\delta(X-X_{ij})\delta(Y-Y_{ij})$ multiplied by the exponential term $\exp\left[j\left(\phi(p)-\frac{2\omega_k R(p)}{c}\right)\right]$ induced by target's mass center radial displacement and along track phase variation. Image reconstruction procedure in its essence is to reveals the 2-D discrete complex reflectivity density function.

4. Image reconstruction algorithm

Target travels several range bins during the observation time due to the translational motion of the mass center on the line of sight (Fig.2). Phase correction algorithm puts each reference point in its initial range bin and compensates for all ISAR signal's phases induced by motion of high order.

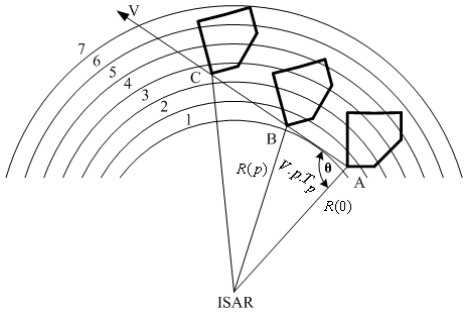

Fig. 2. Traveling of the target trough rang bins.

The image reconstruction procedure does reveal the 2-D discrete complex reflectivity density function. It can be implemented by the following computational operations. First, phase correction of the complex matrix $S(k,p)$ by multiplication with complex conjugated exponential term $\exp\left[-j\left(\phi(p)-\frac{2\omega_k R(p)}{c}\right)\right]$, i.e.

$$\widetilde{S}(k,p)=S(k,p).\exp\left[-j\left(\phi(p)-\frac{2\omega_k R(p)}{c}\right)\right] \quad (15)$$

which can be written as $\widetilde{S}(k,p)=S(k,p).\exp\left[-j\Phi(p)\right]$, where $\Phi(p)=\phi(p)-\frac{2\omega_k R(p)}{c}$, $\exp\left[-j\Phi(p)\right]$ stands for moving compensation function commonly called autofocusing function. The phase correction function $\Phi(p)$ can be expressed by the polynomial expansion

$$\Phi(p)=a_0+a_1 p+a_2 p^2+\ldots+a_n p^n$$

Coefficients can be calculated iteratively using an entropy quality function.

Second, discrete 2-D inverse Fourier transform of phase corrected complex matrix, i.e.

$I(i,j)=\left|\frac{1}{NK}\sum_{p=0}^{N-1}\sum_{k=0}^{K-1}\widetilde{S}(k,p).\exp\left[j\left(\frac{2\pi.p.i}{N}+\frac{2\pi.k.j}{K}\right)\right]\right|$, which can be rewritten as

$$I(i,j)=\left|\frac{1}{NK}\sum_{p=0}^{N-1}\left[\sum_{k=0}^{K-1}\widetilde{S}(k,p).\exp\left(j\frac{2\pi.k.j}{K}\right)\right]\exp\left(j\frac{2\pi.p.i}{N}\right)\right| \quad (16)$$

a. Phase correction based on 2-D Entropy Minimization

After range bin alignment, all the scatterers of the target remain into their initial range bins. In spite of this an unknown phase error is still left in the ISAR signals, which is needed to evaluate.

The autofocusing phase correction is accomplished by multiplication of demodulated ISAR signal data with exponential phase correction function $\exp(-j\Phi)$, i.e.

$$S(p,k)=\hat{S}(p,k)\exp(-j\Phi). \quad (17)$$

After current phase correction define the power normalized image as

$$\bar{I}_{p,k}(\Phi)=\frac{\left|I_{p,k}(\Phi)\right|^2}{\sum_{p=0}^{N-1}\sum_{k=0}^{K-1}\left|I_{p,k}(\Phi)\right|^2}. \quad (18)$$

The image cost function is defined as 2-D entropy function of the normalized ISAR image

$$H(\Phi) = -\sum_{p=0}^{N-1}\sum_{k=0}^{K-1} \bar{I}_{p,k}(\Phi)\ln[I_{p,k}(\Phi)]. \quad (19)$$

The estimate of the phase error function is calculated by minimizing the entropy image cost function

$$\hat{\Phi} = \arg\min_{\Phi}\left\{H[\bar{I}_{p,k}(\Phi)]\right\}. \quad (20)$$

The autofocusing phase correction is accomplished by multiplication of the range compressed ISAR data with exponential phase correction function $\exp[-j\Phi(p)]$, i.e.

$$S(p,k) = \hat{S}(p,k)\exp[-j\hat{\Phi}(p)]. \quad (21)$$

Then the image reconstruction procedure is repeated. Compute the ISAR image, i.e.

$I_{p,k}(\hat{\Phi}(p)) = \mathbf{FFT}_{\dot{p}}(\hat{S}(\dot{p},k))$ and define $\bar{I}_{p,k}(\hat{\Phi}(p))$.

Compute the entropy function value

$$H(\hat{\Phi}(p)) = -\sum_{p=0}^{N-1}\sum_{k=0}^{K-1} \bar{I}_{p,k}(\hat{\Phi}(p)).\ln[\bar{I}_{p,k}(\hat{\Phi}(p))]. \quad (22)$$

The search process continues until $H(\hat{\Phi}(p))$ acquires minimal value in the global minimum.

5. Numerical experimental results

Results from numerical modeling and autofocus image reconstruction are illustrated in Figs. 3 – 6. In Fig. 3 normalized unfocused image of the aircraft F-18 is depicted. It is noticeable double imaging of the target. In Fig 4 an optimal phase correction function is presented. In this case minimum entropy cost function is achieved. In Fig. 5 the evolution of the entropy cost function is illustrated. The minimum value of the achieved entropy cost function is 6.198. In Fig. 6 final focused image of the aircraft F-18 is presented.

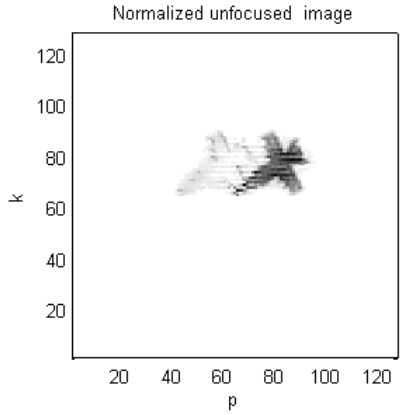

Fig. 3. Normalized unfocused image.

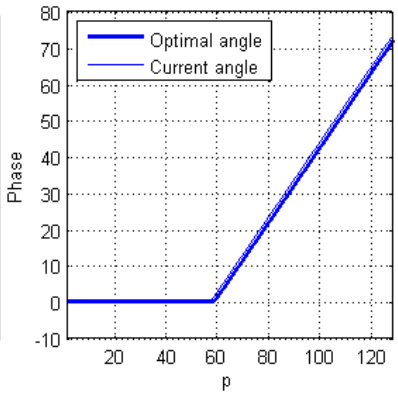

Fig. 4. Optimal phase correction function.

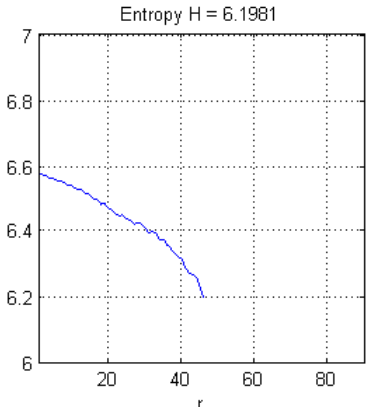

Fig. 5. Evolution of the entropy cost function.

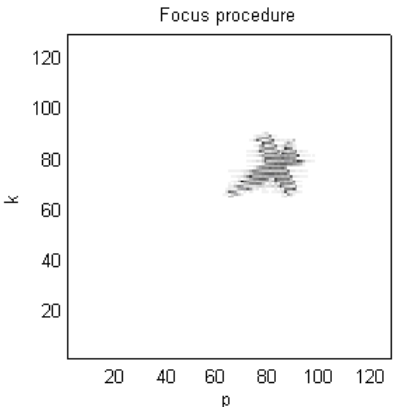

Fig. 6. Final focused image of the aircraft F-18

5. Conclusions

In the paper generalized ISAR geometry and image reconstruction technique have been discussed. ISAR scenario's projection on two-dimensional (2-D) radar registration plane has been considered. The arbitrary movement of the object has been decomposed into two components: radial displacement of the object's geometric center and rotational movement around it. It has been proven that the demodulated ISAR signal, reflected from the target during aperture synthesis, can be considered as 2-D Fourier transformation of the image function, corrected by an exponential term and as a consequence, the image function can be extracted by 2-D inverse Fourier transformation of the phase corrected ISAR signal. In order to validate aforementioned statements numerical experiment is performed.

Acknowledgement

The work is supported by Project: NATO CLG ESP.EAP.CLG.983876, ESA C1P-6051.

References

[1] Berizzi, F. ISAR imaging of targets at low elevation angles. *IEEE Transactions on Aerospace and Electronic Systems*, **37**, 2 (Apr. 2001), 419—435.

[2] Berizzi, F., and Corsini, G. Autofocusing of inverse synthetic aperture radar images using contrast optimization. *IEEE Transactions on Aerospace and Electronic Systems*, **32**, 3 (July 1996), 1185—1191.

[3] Berizzi, F., Dalle Mese, E., and Martorella, M. Performance analysis of a contrast-based ISAR autofocusing algorithm. In *Proceedings of the 2002 IEEE Radar Conference*, Long Beach, CA, Apr. 2002, 200—205.

[4] Xi, L., Giosui, L., and Ni, J. Autofocusing of ISAR images based on entropy minimization. *IEEE Transactions on Aerospace and Electronic Systems*, **35**, 4 (Oct. 1999), 1240 - 1252.

[5] Li, J., Wu, R., and Chen, V. C. Robust autofocus algorithm for ISAR imaging of moving targets. *IEEE Transactions on Aerospace and Electronic Systems*, **37**, 3 (July 2001), 1056 - 1069.

[6] Berizzi, F., Martorella, M., Haywood, B., Dalle Mese, E., and Bruscoli, S. A survey on ISAR autofocusing techniques. In *Proceedings of the IEEE ICIP 2004*, Singapore, Oct. 2004.

[7] Martorella, M., Haywood, B., Berizzi, F., and Dalle Mese, E. Performance analysis of an ISAR contrast based autofocusing algorithm using real data. In *Proceedings of the 2003 IEE Radar Conference*, Adelaide, SA, Australia (Sept. 2003), 200—205.

[8] Martorella, M., F. Berizzi. Time Windowing for Highly Focused ISAR Image Reconstruction, IEEE, Transaction on AES, vol. 41, No3, July 2005.